Endogenous Notch Signaling in Adult Kidneys Maintains Segment-Specific Epithelial Cell Types of the Distal Tubules and Collecting Ducts to Ensure Water Homeostasis

Malini Mukherjee,[1] Jennifer deRiso,[1] Karla Otterpohl,[2] Ishara Ratnayake,[3] Divya Kota,[3] Phil Ahrenkiel,[3] Indra Chandrasekar,[2,4] and Kameswaran Surendran[1,4]

Due to the number of contributing authors, the affiliations are listed at the end of this article.

ABSTRACT

Background Notch signaling is required during kidney development for nephron formation and principal cell fate selection within the collecting ducts. Whether Notch signaling is required in the adult kidney to maintain epithelial diversity, or whether its loss can trigger principal cell transdifferentiation (which could explain acquired diabetes insipidus in patients receiving lithium) is unclear.

Methods To investigate whether loss of Notch signaling can trigger principal cells to lose their identity, we genetically inactivated *Notch1* and *Notch2*, inactivated the Notch signaling target *Hes1*, or induced expression of a Notch signaling inhibitor in all of the nephron segments and collecting ducts in mice after kidney development. We examined renal function and cell type composition of control littermates and mice with conditional Notch signaling inactivation in adult renal epithelia. In addition, we traced the fate of genetically labeled adult kidney collecting duct principal cells after *Hes1* inactivation or lithium treatment.

Results Notch signaling was required for maintenance of Aqp2-expressing cells in distal nephron and collecting duct segments in adult kidneys. Fate tracing revealed mature principal cells in the inner stripe of the outer medulla converted to intercalated cells after genetic inactivation of *Hes1* and, to a lesser extent, lithium treatment. *Hes1* ensured repression of *Foxi1* to prevent the intercalated cell program from turning on in mature Aqp2$^+$ cell types.

Conclusions Notch signaling *via Hes1* regulates maintenance of mature renal epithelial cell states. Loss of Notch signaling or use of lithium can trigger transdifferentiation of mature principal cells to intercalated cells in adult kidneys.

J Am Soc Nephrol 30: 110–126, 2019. doi: https://doi.org/10.1681/ASN.2018040440

Multicellular organisms are dependent on the development and maintenance of diverse cell types in order to remain healthy. Considering the potential plasticity of mature cells,[1] a disease may arise from the disruption of a molecular mechanism that ensures the stability of a mature cell state. In organs such as the kidneys, which comprise diverse cell types, mechanisms must be in place to maintain diverse epithelial cell types and prevent cells from switching between cell types. Cell type conversion is hypothesized to occur within adult kidney collecting ducts of patients on lithium therapy for treatment of bipolar disorders and can result in acquired nephrogenic diabetes insipidus (NDI), which involves a urine-concentrating defect. Furthermore, long-term lithium usage increases the likelihood of developing ESRD by at least six-fold.[2]

Received April 27, 2018. Accepted November 7, 2018.

Published online ahead of print. Publication date available at www.jasn.org.

Correspondence: Dr. Kameswaran Surendran, Pediatrics and Rare Diseases Group, Sanford Research, 2301 E 60th Street N, Sioux Falls, SD 57104. Email: kameswaran.surendran@sanfordhealth.org

Whether lithium triggers conversion of principal cells (PCs), which are required for water reabsorption, into intercalated cells (ICs) that predominantly contribute to pH regulation remains to be determined. In support of the lithium-induced conversion of cell types, rodent models of lithium-induced NDI and recovery of the kidney after lithium withdrawal have provided evidence for the existence of a transitional cell type with properties of both intercalated and PC types.[3] However, definitive evidence for conversion of PCs to ICs or *vice versa* is needed, and the molecular mechanisms that regulate this hypothesized switch in adult cell types remain unknown.

The kidney collecting ducts develop from the ureteric bud as a branched network of tubular structures comprising multiple epithelial cell types critical for water, electrolyte, and pH homeostasis. The ureteric bud repeatedly branches giving rise to the collecting duct system, which, in the mature state, contains ICs and PCs.[4] The PCs uniquely express aquaporin-2 (Aqp2) apically and arginine-vasopressin receptor-2 (Avpr2), aquaporin-3 (Aqp3) and aquaporin-4 (Aqp4) on the basolateral membranes and are responsive to arginine vasopressin peptide to regulate water homeostasis.[5] The ICs are responsible for pH homeostasis, protection against bacterial infection of the urinary system,[6] and express carbonic anhydrases, vacuolar H^+-ATPase pumps, and anion exchangers (AEs).[7–9] On the basis of the differential localization of vacuolar H^+-ATPase and the type and localization of AEs (apical versus basolateral), ICs are classified into type A, B, or non-A-non-B[10–14] ICs that belong to an evolutionarily conserved cell type referred to as proton-secreting cells or ionocytes[15] found in many mammalian organ systems, including the connecting segment and collecting ducts of kidneys, inner ear, and epididymis. The differentiation of proton-secreting cells in *Xenopus* and zebrafish skins and the mammalian kidney collecting ducts is promoted by *Foxi1* orthologs, and negatively regulated by Notch signaling.[16–20] Additionally, grainyhead transcription factors are critical for IC development.[16,21] More recently, single-cell RNA-sequencing of mouse cortical kidney collecting duct cell types has revealed a more comprehensive list of components of PCs and ICs, including the confirmation that *Notch2* mRNA is enriched in PCs whereas *Jag1* mRNA, coding for a Notch ligand, is enriched in ICs.[22]

Inactivation of Notch signaling during kidney collecting duct development aberrantly favors differentiation of collecting duct cells into ICs instead of PCs, resulting in an NDI-like phenotype.[18,20,23] The development of an insufficient number of PCs reduces the renal urine concentrating capacity. Intriguingly, an alteration in PC-to-IC ratio also occurs in rodents treated with lithium or inactivation of *dot1l*.[3,24–26] The underlying mechanism by which lithium alters collecting duct cell types remains unclear.[27] Here, we test the hypotheses that loss of Notch signaling, or lithium treatment, can independently trigger PCs in adult kidneys to lose their identity. We have determined that in the adult kidney connecting tubule (CNT) and collecting duct segments, where different types of epithelial cells coexist intermingled within segments, Notch signaling maintains epithelial cell type diversity by preventing transdifferentiation of the majority cell type into the neighboring minority cell type.

Significance Statement

Although plasticity of mature cells has potential advantages, appropriate maintenance of functionally diverse cell types in organized structures, such as the kidney, is essential. Notch signaling is required for normal kidney development, including principal cell fate selection, but inappropriate activation of Notch in adult kidneys promotes CKD progression. In this study, the authors describe a novel physiologic requirement for endogenous Notch signaling in adult kidneys: preventing mature aquaporin-2–expressing epithelial cell types in the connecting segment and collecting ducts from directly converting into ionocytes, or intercalated cells. The authors' findings indicate that maintenance of mature epithelial cell types is an active process, and identify inappropriate transdifferentiation between epithelial cell types as a possible underlying cause of disease, such as acquired nephrogenic diabetes insipidus.

METHODS

Mice

All experiments involving mice were approved by the Sanford Research Institutional Animal Care and Use Committee. All mouse lines used in this study have been previously described and are listed in Supplemental Table 1 and were maintained on mixed backgrounds. Mice were genotyped following a universal PCR genotyping protocol.[28] Primer sequences are available upon request. Doxycycline (dox; 1 mg/ml; Sigma-Aldrich) and bromodeoxyuridine (BrdU; 1 mg/ml; Fisher Scientific) were administered in drinking water containing 5% sucrose to adult mice during which they continued to be fed normal chow *ad libitum*. Wild-type control groups consisted of age- and, where possible, sex-matched littermates housed along with mice with conditional inactivation of Notch signaling. We initiated inactivation of floxed alleles of *Notch1* and *Notch2* (*N1 f/f; N2 f/f*) or *Hes1* (*Hes1f/f*) genes using Pax8 transgene driving reverse tetracycline transactivator (*Pax8->rtTA*) and a tetracycline response element (*TRE*) driving the expression of Cre (*TRE->Cre*) in 3-week-old mouse nephrons and collecting ducts. We compared *Pax8->rtTA; TRE->Cre; N1f/f; N2*/f* mice (*Notch1* and *Notch2 cKO*), where * denotes floxed or deleted allele, with wild-type control littermates: *TRE->Cre; N1f/f;N2*/f*, *Pax8->rtTA; N1f/f;N2*/f* and *N1f/f;N2*/f* mice. Similarly, we compared *Pax8->rtTA; TRE->Cre; Hes1f/f* (*Hes1cKO*) mice with wild-type control littermates consisting of *TRE->Cre; Hes1f/f*, *Pax8->rtTA; Hes1f/f*, and *Hes1f/f* genotypes. We observed no significant differences between males and females of the same genotype and therefore included both sexes in analyses of wild-type versus mutant groups. The lithium diet consisting of 40 mmol of lithium chloride per kilogram of mouse dry chow (Munson Lakes Nutrition) was provided for 2 weeks *ad libitum*. Twenty four hour mouse urine samples were collected by housing mice individually in

metabolic cages. The urine osmolality was determined using a VAPRO Vapor Pressure Osmometer (WESCOR).

Histology and Immunohistochemistry

Kidneys were perfusion-fixed using 4% PFA/0.1 M cacodylate (Figures 6 and 7), or immersion fixed in 4% PFA or Bouin fixative (Figures 1–5) overnight at 4°C, washed in 70% ethanol, paraffin-embedded, and sectioned at 12 μm thickness. Before immunostaining, the sections were deparaffinized in xylene, rehydrated, and boiled for 20 minutes in Trilogy (Cell Marque) for antigen unmasking. Sections were blocked in PBS containing 1% BSA, 0.2% powdered skim milk, and 0.3% Triton X-100 for at least 15 minutes at room temperature before incubation with primary antibodies overnight. For direct visualization of GFP or tdtomato, the mouse kidneys were fixed in 4% PFA for 1 hour, rinsed in PBS, and incubated in 15% sucrose for 24 hours, and then for another 24 hours in 30% sucrose before embedding in OCT and sectioning at 12 μm thickness. Supplemental Table 2 lists the primary antibodies used in this study. Secondary antibodies conjugated with DyLight405, Alexa Fluor 488, Cy3, and Cy5 (Jackson ImmunoResearch) were used at 1:500 dilution to visualize the primary antibodies. Coverslips were mounted using the VECTASHIELD fluorescence mounting media with or without DAPI (Vector Laboratories), and sealed using nail polish. Some tissue sections were counterstained with Hoechst dye instead of DAPI. Stained tissue sections were imaged on a Nikon A1 confocal microscope using NIS elements software for image acquisition.

Lineage Tracing Analysis and BrdU Counting

Elf5->rtTA;Tet-O-Cre; Rosa$^{+/tdtomato}$ mice with or without Hes1$^{f/f}$ were administered 1 mg/ml dox in the drinking water from 3 to 5 weeks of age, to turn on tdtomato expression in Elf5-expressing collecting duct cells. These mice were perfusion-fixed using 4% PFA/0.1 M cacodylate at 6 weeks of age. A separate cohort of *Elf5->rtTA;Tet-O-Cre; Rosa*$^{+/tdtomato}$ mice were administered 1 mg/ml dox in the drinking water from 3 to 5 weeks of age, and then given normal diet or lithium diet consisting of 40 mmol lithium chloride per kilogram of mouse dry chow, from 6 to 8 weeks of age *ad libitum*, and perfusion-fixed using 4% PFA/0.1 M cacodylate at 8 weeks of age. At least 150 tdtomato$^+$ medullary collecting duct cells were analyzed for expression of cell type marker per mouse kidney to determine the percentage of tdtomato$^+$ medullary collecting duct cells that expressed PC or IC markers. A one-way ANOVA was performed to compare three Hes1-deficient mouse kidneys with four control kidneys and three lithium-treated mouse kidneys. For BrdU counting, BrdU was provided in the drinking water along with dox from 3 to 5 weeks of age, to *Pax8->rtTA; TRE->Cre; Hes1f/f* mice and control littermates (n=4 per genotype). These mice were perfusion fixed using 4% PFA/0.1 M cacodylate and the kidneys and small intestines were harvested. The small intestines were analyzed to ensure incorporation of BrdU in the intestinal epithelial cells. At least 1400 cells of the inner stripes of the outer medullary collecting duct (OMCD) were analyzed per mouse for expression of Aqp4, c-Kit, and incorporation of BrdU.

Three-Dimensional Image Generation and Determination of Cell Type per Tubule Length

Four-week-old *Hes1cKO* mice (1 week after initiation of *Hes1* inactivation) and control littermates were perfusion fixed using 4% PFA/0.1 M cacodylate solution and harvested kidneys were vibratome sectioned at 100 μm before staining with Foxi1, Aqp4, and Hoechst for three-dimensional image generation. Confocal Z-stack images (optical sections) were captured every 0.175 μm using a $\times$60 objective on a Nikon A1 confocal microscope. The Z-stacks were converted to Maximum Intensity Projections, or movies for three-dimensional visualization and ISO surface visualization by three-/four-dimensional image processing software called Arivis Vision 4D (Arivis AG, Munich, Germany). A minimum of seven inner stripe outer medullary duct segments were analyzed to determine the average number of each cell type per tubule length per mouse. Cells with only nuclear Foxi1 were counted as intercalated, cells with basal Aqp4 were counted as principal, and cells with nuclear Foxi1 and obvious basal Aqp4 were counted as intermediate cells. These counts may be underestimating the number of intermediate cells in the *Hes1cKO*, as we counted Foxi1$^+$ cells as intercalated and not intermediate cells if we had any doubt about whether the Aqp4 signal next to nuclear Foxi1 was from the same cell or a neighboring cell. Three mice per genotypic group were analyzed to determine the average number of each cell type per 100-μm tubule length for each genotype.

Cell Type Composition of Tubule Segments

The percentage of each cell type in the distal convoluted tubule segment 2 (DCT2) and connecting tubule (CNT) were determined using five mice per genotype. The percentage of each cell type in cortical collecting duct (CCD), inner stripe of the OMCD, and initial part of the inner medullary collecting duct (IMCD) were determined using three mice per genotype. CCD were identified on the basis of cortical location, presence of glomeruli in the region, and/or close proximity to calbindinD-expressing tubule segments (Supplemental Figure 1, C and D), and were differentiated from CNT and DCT2 on the basis of presence of Aqp2 expression and absence of calbindinD expression. The presence (cortex) versus absence (noncortex) of calbindinD-positive tubule segments served to distinguish between the cortex and medulla (Supplemental Figure 1). OMCD segment counts excluded the outer stripes and are enriched for inner stripes of the OMCDs (Supplemental Figure 1). Throughout this article, OMCD refers to the inner stripe of the OMCD. We made use of the density of collecting duct rays in the inner stripe of the outer medulla being more sparse compared with the collecting ducts in the inner medulla, to distinguish between the OMCD and IMCD (Supplemental Figure 1). The inner stripe of the outer

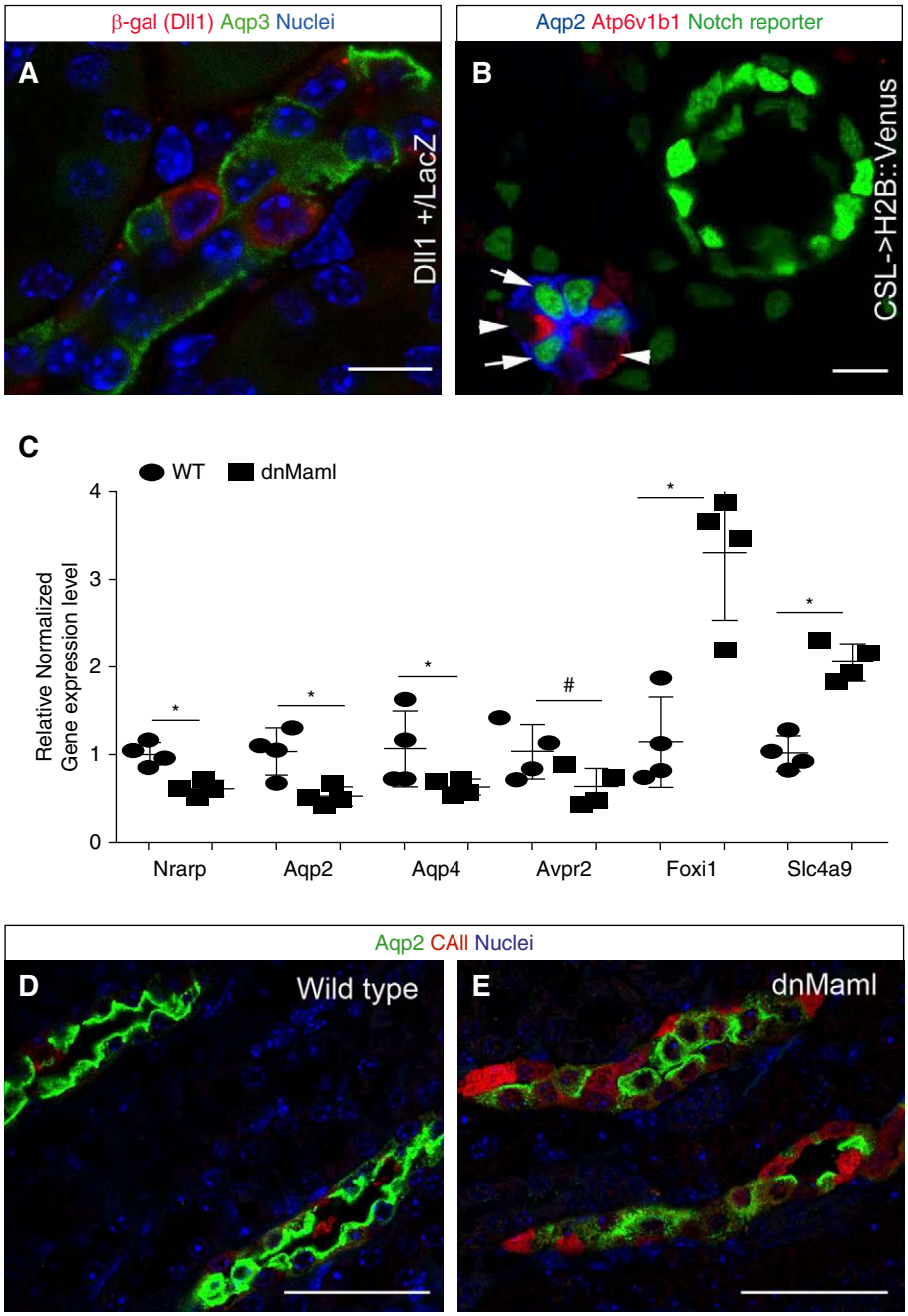

Figure 1. Active Notch signaling occurs after development in mouse kidneys and is required for maintaining PC gene expression and function. (A) The Notch ligand Delta-like 1 (Dll1) continues to be expressed in the inner stripe of the OMCD cells adjacent to Aqp3^{+} cells as determined by β-galactosidase staining (red) in Dll1$^{+/LacZ}$ mice. (B) The Notch reporter CBF->H2B::Venus reveals continued Notch signaling in adult mouse kidneys, including the CCDs. Arrows indicate cells with nuclear H2B::Venus and cell membrane localization of Aqp2, and arrowheads are pointing at Atp6v1b1-expressing intercalated cells. (C) Dox-induced expression of dnMaml in adult nephrons and collecting ducts leads to suppression of Notch pathway target (*Nrarp*) and PC genes (*Aqp2, Aqp4, Avpr2*) and induction of intercalated cell genes (*Foxi1, Slc4a9*) in whole kidneys after 3 days of dox treatment. n=4 per group; *P<0.05; $^{\#}P$=0.073, two-tailed unpaired t test. (D and E) The inner stripe of the outer medullary regions of kidneys with inhibited Notch signaling (E) show an increase in CAII and a decrease in PC marker Aqp2 when compared with wild-type littermates (D). (F) Mice with dox induced dnMaml expression in nephrons and collecting ducts show reduced 24-hour urine osmolality compared with wild-type littermates. Differences are statistically significant after 3 days (n=4 wild-type versus 5 dnMaml mice, *$P<1.7\times10^{-3}$, two-tailed unpaired t test) and after 7 days (n=3 wild-type versus 4 dnMaml mice, * $P<2.3\times10^{-4}$, two-tailed unpaired t test) of dox treatment. Scale bars, 10 μm in (A and B), and 50 μm in (D and E).

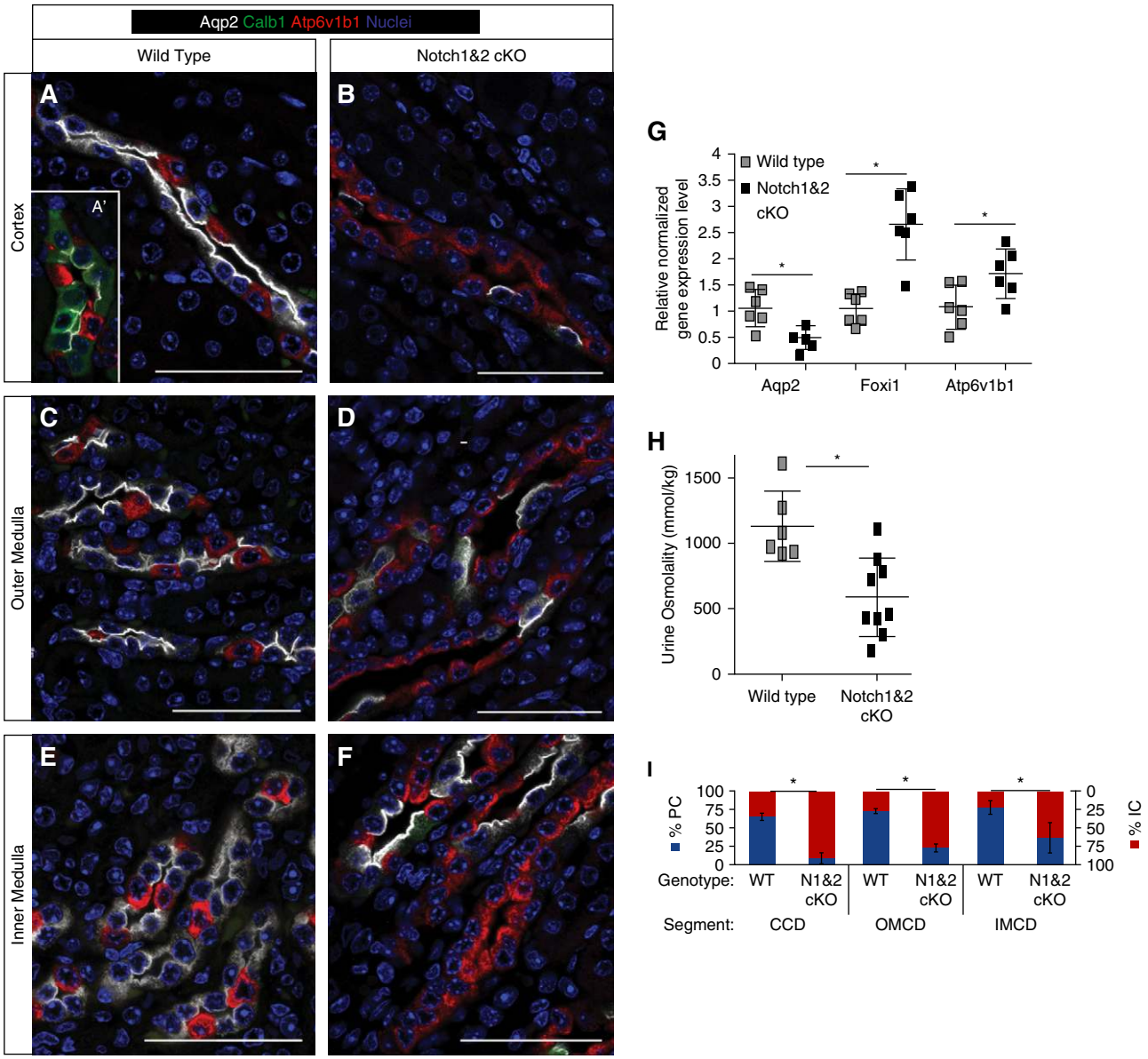

Figure 2. *Notch1* and *Notch2* are required for maintenance of PC identity and proper functioning of the collecting ducts. (A–F) Kidneys from 8-week-old mice with conditional inactivation of *Notch1* and *Notch2* (*Notch1 & 2 cKO*) in the renal tubules and collecting ducts (B, D, and F) beginning at 3 weeks of age show reduced number of Aqp2-expessing (white) PCs when compared with wild-type littermates (A, C, and E). *Notch1 & 2 cKO* mouse kidneys also show an increase of ATP6v1b1-expressing (red) intercalated cells in the CCDs (B), inner stripe of the OMCDs (D), and the initial IMCDs (F) when compared with wild-type CCD (A), OMCD (C), and IMCD (E). CCDs do not express calbindin1 (green) and are different from CNT, which express both calbindin1 and Aqp2 (A'). Scale bars, 50 μm. (G) Quantitative RT-PCR using RNA extracted from whole kidneys reveals reduced levels of Aqp2 and increased levels of Foxi1 and Atp6v1b1 in Notch1 & 2 cKO versus wild type at 8 weeks of age (*$P<0.05$, $n=6$ per group, two-tailed unpaired t test). (H) At 8 weeks, there is a significant decrease in the urine-concentrating ability of *Notch1 & 2 cKO* mice (*$P<0.00$, $n=6$ wild-type versus 9 *Notch1 & 2 cKO* mice, two-tailed unpaired t test). (I) The average percentage of PCs (height of blue bar) and ICs (red bar) along with one SD (error bars) is depicted for the CCD, OMCD, and IMCD in wild-type (WT) versus *Notch1 & 2cKO* (N1 & 2cKO). Two-tailed unpaired t tests reveal that the average %PC is decreased in the N1 & 2cKO in each of collecting duct segments when compared with that of WT kidneys (*$P<0.05$, $n=3$ mice per group, at least 100 cells were counted per collecting duct segment per kidney).

medullary region still contains the thick ascending and the thin descending limb of the loop of Henle, whereas we considered the initial part of the inner medullary region as the region containing the thin ascending and thin descending limbs of the loop of Henle (Supplemental Figure 1). The IMCDs we counted were in the initial part of the inner medullary region in which noncollecting duct (Aqp2-negative) tubules were still interspersed between the collecting

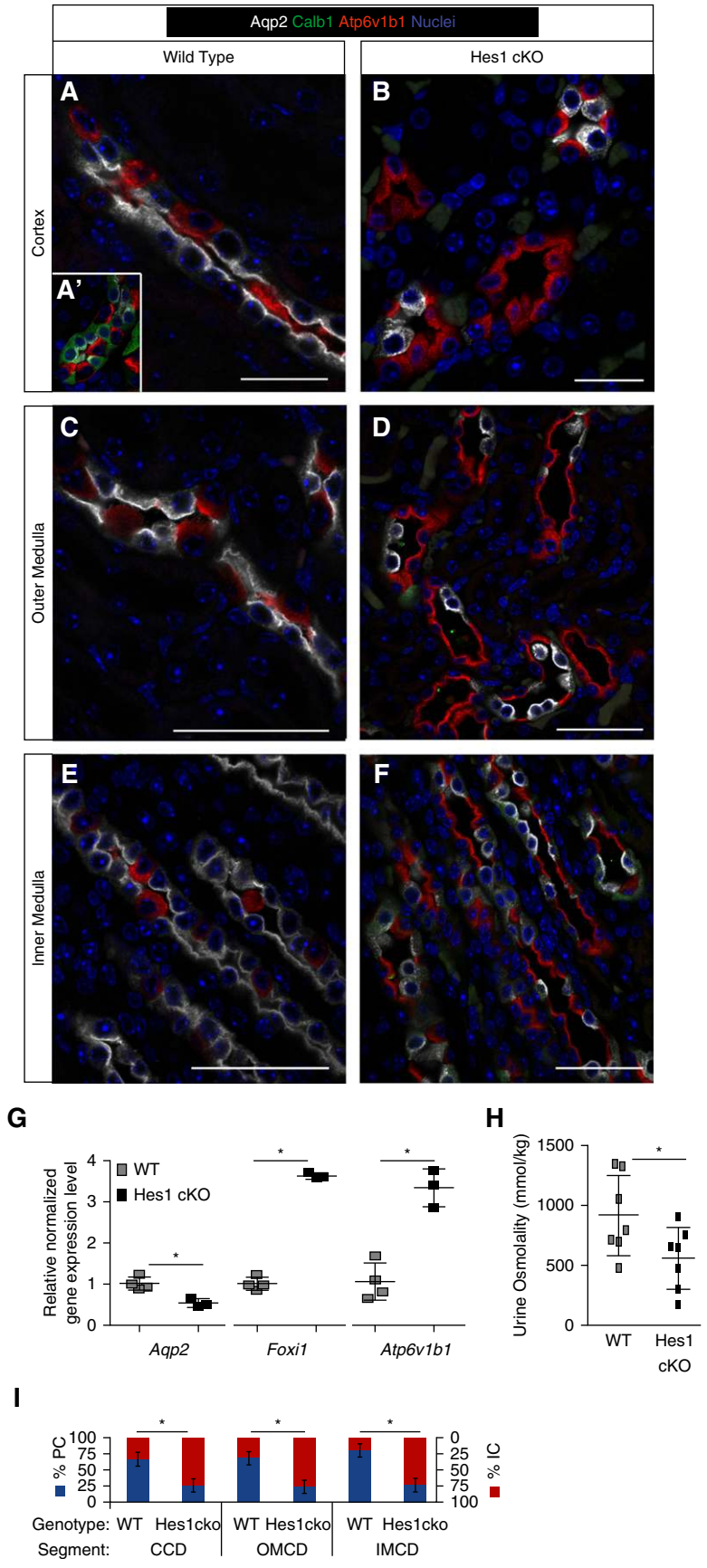

ducts. We excluded the IMCD segments that did not contain intercalated cells and those that did not have noncollecting duct (Aqp2-negative) tubule segments neighboring them from the IMCD counts. At least 100 cells were counted per segment per mouse, using ×60 images captured using Nikon A1 confocal. Individual cells were identified by the presence of a visible nucleus and/or basolateral membranes, and then assigned a cell type on the basis of the presence of Aqp2, calbindinD, and Atp6v1b1. Cells with ambiguous marker staining or no marker staining were excluded from the counts.

RNA *In Situ* Hybridization Using RNAscope and Basescope

Mice were perfused using 4% PFA/0.1 M cacodylate solution and harvested kidneys were incubated in 15% sucrose overnight, followed by 30% sucrose overnight. Kidneys were frozen in OCT solution and sectioned at 10 μm onto Superfrost Plus slides.

Figure 3. *Hes1* is critical for the maintenance of PC identity and function. (A–F) Kidneys from 8-week-old mice with dox-induced conditional inactivation of *Hes1* (*Hes1cKO*) in the renal tubules and collecting ducts from 3 weeks of age show reduced number of Aqp2-expessing (white) PCs (B, D, and F) when compared with wild-type littermates (A, C, and E) in the cortex, inner stripe of the outer medulla, and initial part of the inner medulla. In the cortex, the CCDs were distinguished from CNTs on the basis of the presence of calbindin1 in CNT and not CCD (A'). *Hes1cKO* kidneys have increased Atp6v1b1-expressing (red) intercalated cells. Scale bars, 25 μm (A and B) and 50 μm (C–F). (G) Quantitative RT-PCR of RNA from whole kidneys reveals reduced *Aqp2* and increased *Foxi1* and *Atp6v1b1* in *Hes1cKO* versus wild type 1 week after dox initiation. (*$P<0.05$, $n=4$ wild type and 3 Hes1cKO, two-tailed unpaired *t* test). (H) At 8 weeks, there is a significant decrease in the urine-concentrating ability of *Hes1cKO* mice ($n=7$) versus wild type ($n=7$); *$P=0.05$, two-tailed unpaired *t* test. (I) Two-tailed unpaired *t* tests reveal that the average %PC is decreased in the *Hes1cKO* in each of the collecting duct segments when compared with that of wild-type kidneys (*$P<0.05$, $n=3$ mice per group, at least 100 cells were counted per collecting duct segment per kidney).

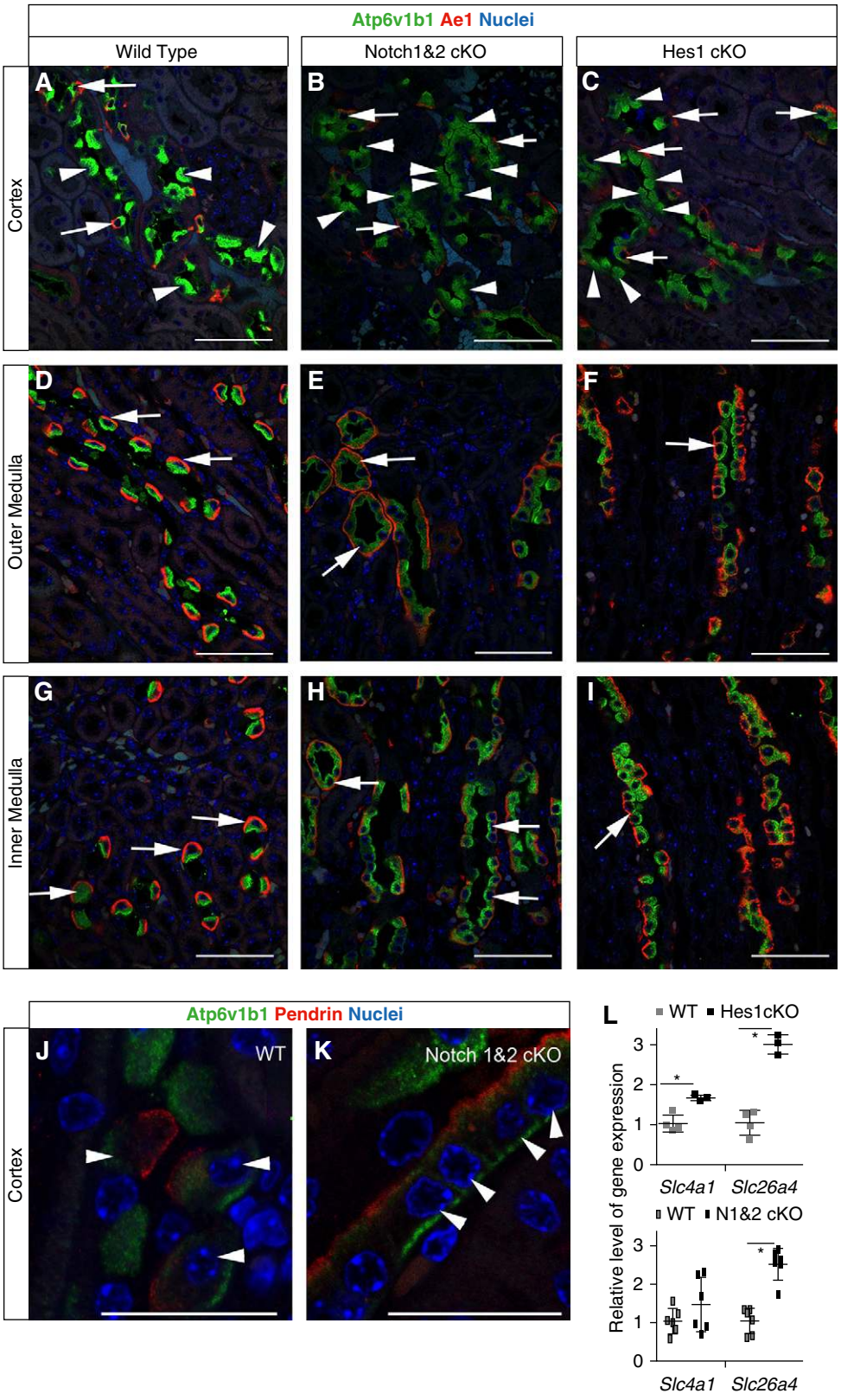

Figure 4. Loss of Notch signaling triggers an increase primarily in pendrin-expressing intercalated cells in the cortex, and type A intercalated cells in the outer and inner medullary regions. (A, D, and G). Wild-type mouse kidneys show relatively few type A intercalated cells in the cortex, as identified by basolateral expression of AE-1 (arrows in A), compared with inner stripe of the outer medullary and initial inner medullary regions (arrows in D and G, respectively). (B and C) Conditional inactivation of *Notch1* and *Notch2*

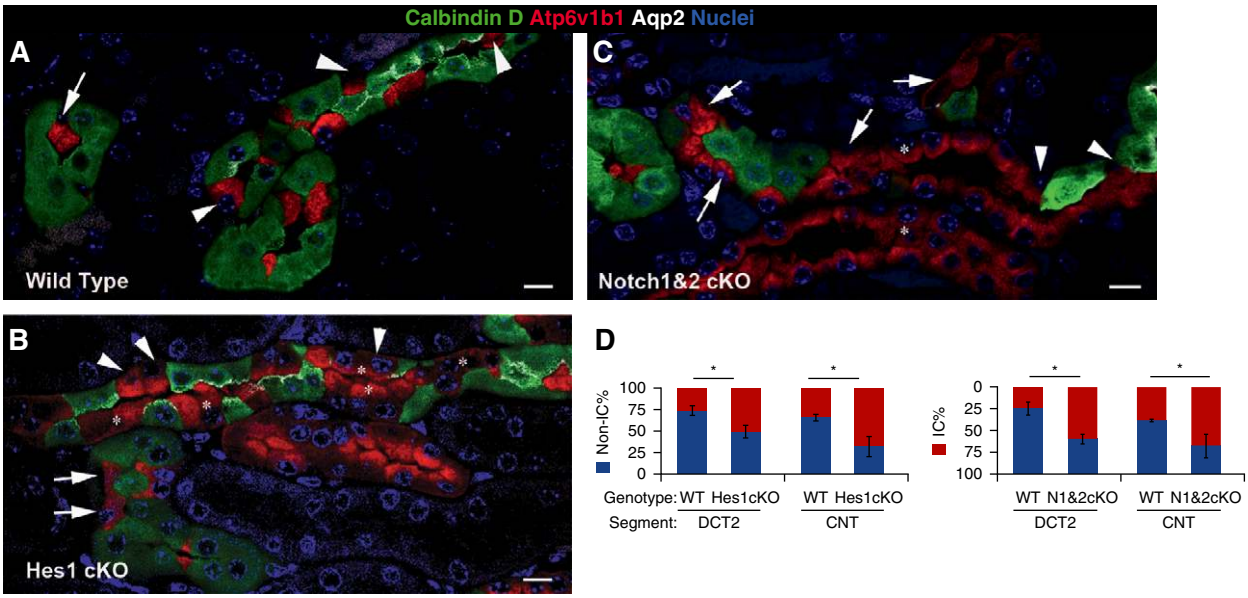

Figure 5. Notch signaling is required for the maintenance of Aqp2-expressing cells in the CNTs of distal nephrons. (A) Arrowheads point to examples of individual Atp6v1b1$^+$ intercalated cells in wild-type CNT that are surrounded by cells expressing both Calb1 and Aqp2. Arrow points to Atp6v1b1$^+$ intercalated cell surrounded by cells expressing Calb1 and not Aqp2 in the DCT2. (B and C) In both *Notch1 & 2 cKO* and *Hes1cKO*, the number of Atp6v1b1$^+$ intercalated cells are increased in the CNT and DCT2 compared with wild-type CNT and DCT2. Stretches of Atp6v1b1$^+$ cells are frequently observed (asterisks) in the absence of Notch signaling. Scale bars, 10 μm. (D) The average percentage of non-ICs (height of blue bar) and ICs (red bar) along with one SD (error bars) is depicted for the CNT and DCT2 in wild type (WT) versus Hes1cKO and WT versus Notch1 & 2cKO (N1 & 2cKO). Two-tailed unpaired *t* tests reveal that the average %non-IC is decreased in the Notch signaling–deficient kidneys in each of the subsegments when compared with that of WT kidneys (*$P<0.05$, $n=5$ mice per group, at least 100 cells were counted per tubule subsegment per kidney).

RNAscope and Basescope assays were performed using RNAscope Multiplex Fluorescent Reagent Kit v2 and Basescope Detection Reagent Kit v2-RED, respectively (Advanced Cell Diagnostics). Tissue sections on slide were fixed in 4% PFA for 90 minutes at room temperature, followed by dehydration in alcohol series and H_2O_2 pretreatment for 10 minutes at room temperature. Sections were then boiled in 1× antigen retrieval solution for 15 minutes, washed in 100% ethanol for 5 minutes, and air dried. The next day, sections were treated with Protease Plus for 30 minutes, at 40°C in HybEZ Oven (Advanced Cell Diagnostics). Probes specific to Hes1 or Notch2 (targeting only the deleted exons) were applied for 2 hours at 40°C. Sections were then washed and the signal was amplified according to manufacturer's instructions (AMP1-AMP3 for RNAscope, AMP1-AMP8 for Basescope). For RNAscope samples, probe-specific signal was developed with HRP-C1 for 15 minutes at 40°C, followed by amplification with TSA Plus-Fluorescein (1:900) (Perkin Elmer). Sections were then washed and treated with HRP blocker. For immunofluorescence staining of collecting duct marker cytokeratin8, sections were blocked for 30 minutes in TBS-1% BSA buffer at room temperature. Cytokeratin8 antibody (1:20) was applied for 1 hour. Sections were then washed for 5 minutes 3× at room temperature, in TBST. HRP-conjugated secondary antibody (1:500) was applied for 30 minutes, and the HRP signal was amplified with 1:300 TSA plus cyanine3, for 15 minutes at room temperature. For Basescope detection, after AMP8 treatment, slides were washed 2× for 5 minutes, and the signal was developed with 1:60 mix of Basescope Fast RED-B to Fast RED-A for 10 minutes at room temperature. Slides were then washed with tap water 5 minutes. For immunofluorescence staining, sections were blocked in PBS with 0.15% Triton X-100,

or *Hes1* increases the number of AE-1-negative intercalated cells in the cortex (arrowheads), whereas the type A intercalated cells are present in numbers comparable with that in wild-type kidneys (arrows). (E, F, H, and I) Rows of type A intercalated cells (arrows) are present in *Notch1 & 2cKO* and *Hes1cKO* inner stripe of the outer medulla (E and F) and the initial part of the inner medulla (H and I), accounting for almost all of the increase in intercalated cells in these regions. (J and K) Pendrin-expressing intercalated cells (arrowheads) are increased in the cortex of *Notch1 & 2cKO* kidneys (K) compared with that of wild-type kidneys (J). Scale bars, 50 μm, except in (J and K), which are 25 μm. (L) Quantitative RT-PCR reveals increased expression of *Slc4a1* and *Slc26a4* in Hes1cKO kidneys 1 week after dox initiation (*$P<0.05$, *t* test $n=4$ wild type and 3 *Hes1cKO*). There is also a significantly higher level of *Slc26a4* expression and a trend toward increased expression of *Slc4a1* in 8-week-old *N1 & 2cKO* kidneys versus control littermates (*$P<0.05$, $n=6$ per group).

followed by primary antibody staining for 1 hour at room temperature, secondary antibody (1:500 Alexa Fluor 488 conjugated) for 1 hour at room temperature, without any further amplification.

Electron Microscopy

For electron microscopy, kidney tissues were perfusion fixed using 2% PFA and 2.5% glutaraldehyde in 0.1 M cacodylate solution, followed by fixation with 0.5% OsO_4 plus 0.5% potassium ferrocyanide for 15 minutes. After incubation with 0.2% tannic acid for 30 minutes, the tissues were incubated in 50 mM uranyl acetate in acetate buffer for 15 minutes. Dehydration and embedding in araldite was carried out using conventional procedures. Thin sections of 70 nm were cut with an ultramicrotome (RMC powertome XL) and images were taken on a JOEL 2100 transmission electron microscope.

Quantitative PCR

Flash-frozen whole mouse kidneys were homogenized using a tissue homogenizer (Biospec Products, Inc.). Total RNA was extracted from a portion of the whole kidney lysate using RNeasy Midi-Kit (Qiagen) according to manufacturer's instructions. One microgram of RNA was reverse-transcribed using oligo(dT) with Goscript reverse transcription kit (Promega). For each primer pair, standard curves were generated with serially diluted complementary DNA reverse-transcribed from whole mouse kidneys to determine the efficiency of each primer pair. Each sample was measured in duplicate and the relative gene expression levels were normalized to that of *GAPDH*. For genes expressed at low levels, to avoid sampling error, 5 μg total kidney RNA was reverse-transcribed using a combination of a housekeeping and one or two target gene–specific reverse primers. The resultant complementary DNA was used undiluted for quantitative RT-PCR. Primer sequences are available upon request. The relative expression levels were determined using the $\Delta\Delta$Ct method.[29]

Statistical Analyses

Microsoft Excel was used to perform two-tailed unpaired *t* tests, after testing for equal variance between groups using the *F* test unless stated otherwise. The resulting *P* values are stated in the text and/or figure legends. R (version 3.4.1) was used for one-way ANOVA and *post hoc* pairwise analysis. Our initial comparison of urine osmolality of three wild-type versus four Notch signaling–deficient (*Pax8->rtTA;TRE->dnMaml*) adult mice revealed these numbers were sufficient to detect significant differences between the two groups by two-tailed *t* test, with α=0.05, resulting in an effect size of 7.2 and power of >0.99. For subsequent experiments we therefore continued with *n*=3–9 per group, with the exact numbers depending on the size of, and genotype within, the litters. In the graphs, the height of each bar represents the mean and the error bars represent one SD.

RESULTS

Induction of Dominant-Negative Mastermind-Like-1 Expression in Adult Renal Epithelia Alters the Cell Type Composition of Kidney Collecting Ducts and Diminishes Urine Concentrating Capacity

Adult mouse kidney collecting ducts express the Notch ligand Delta-like-1 (Dll1) in ICs adjacent to Aqp3$^+$ PCs (Figure 1A). Consistent with active Notch signaling in adult collecting ducts, we observed H2B::Venus$^+$ PCs in adult Notch reporter mice[30] (Figure 1B). To determine if Notch signaling is required for maintenance of mature collecting duct cell types, expression of dominant-negative mastermind-like-1 (dnMaml), an inhibitor of Notch signaling–mediated transcription,[31] was induced in nephrons and collecting ducts of 3- to 4-week-old *Pax8->rtTA;TRE->dnMaml* mice by dox treatment.[32–34] Consistent with inhibition of Notch signaling, the expression level of *Nrarp*, a target of Notch signaling,[35,36] is reduced after dox treatment (Figure 1C). Induction of dnMaml reduced expression levels of PC genes *Aqp2*, *Aqp4*, and *Avpr2*, and increased levels of IC-specific genes *Foxi1* and *Slc4a9* (Figure 1C). Consistent with altered intercalated and PC-specific gene expression levels, the number of CAII$^+$ ICs increased and Aqp2$^+$ PCs decreased with dnMaml expression (Figure 1D). Along with changes in collecting duct cell types and gene expression levels, we detected reduced 24-hour urine osmolality in mice with dnMaml induction as early as 3 days after dox treatment compared with dox-treated controls (Figure 1F).

Inactivation of *Notch1* and *Notch2*, or *Hes1*, in Adult Kidneys Triggers Loss of PCs and Gain of Intercalated Cell Types

Although dnMaml blocks Notch signaling–mediated transcription,[31] it is possible that the adult kidney phenotype with induction of dnMaml operates through a mechanism independent of blocking Notch signaling. To confirm the requirement of Notch signaling in adult kidneys, floxed alleles of *Notch1* and *Notch2* (*N1f/f;N2f/f*) were inactivated using *Pax8->rtTA;TRE->Cre* system in 3-week-old mouse nephrons and collecting ducts. Dox treatment of *Pax8->rtTA;TRE->Cre; N1f/f; N2*/f* mice (*Notch1 & 2 cKO*), where * denotes floxed or deleted allele, from 3 to 5 weeks of age resulted in a severe urine concentrating deficit by 8 weeks of age (*n*=6 controls; n=*9 Notch1 & 2 cKO*; Figure 2H). Because Notch signaling is critical for nephron formation and proximal tubule specification during kidney development,[37,38] we examined the proximal tubules in *Notch1 & 2cKO* mice, but did not observe any obvious morphologic changes or significant changes in the expression levels of proximal tubule specific genes, such as megalin, in the kidneys of *Notch1 & 2 cKO* 8-week-old mice (data not shown). Instead, we observed that the *Notch1 & 2 cKO* kidneys have increased Atp6v1b1$^+$ ICs in the CCDs, inner stripes of OMCDs, and in the initial IMCDs compared with that of control kidneys (Figure 2, A–F and I). The increase in ICs is further supported by increased mRNA levels of *Foxi1*

and *Atp6v1b1* in the whole *Notch1 & 2 cKO* kidneys compared with wild-type controls (Figure 2G). The increase in ICs accompanies a decrease in PCs, as evidenced by fewer $Aqp2^+$ cells (Figure 2, A–F and I). All collecting duct segments had fewer PCs in *Notch1 & 2 cKO* kidneys, except for those in the papillary regions (inner two thirds of the inner medulla), which were not noticeably different from control kidneys (data not shown). This does not appear to be due to inefficient inactivation in the papillary region as we detected very few papillary collecting duct cells with Notch2 mRNA in *Notch1 & 2 cKO* kidneys compared with wild-type controls (Supplemental Figure 2). The decrease in PCs was further confirmed using Aqp4 as a PC marker (Supplemental Figure 3) and by the overall reduction in *Aqp2* mRNA levels (Figure 2G). Next, we stained for markers of mitochondria as they are more abundant in ICs than in PCs. Staining for mitochondrial markers CoxIV and Cytochrome C (Supplemental Figure 3) revealed their abundance within Aqp4-negative ICs and not as much in $Aqp4^+$ PCs in control kidneys. In *Notch1 & 2 cKO* kidneys, most of Aqp4-negative duct cells expressed abundant amounts of mitochondrial markers, and most $Aqp4^+$ duct cells had very few mitochondria (Supplemental Figure 3). TEM of *Notch1 & 2 cKO* kidney sections reveals that the increased number of ICs contain many more mitochondria compared with the PCs in the inner stripes of OMCDs (Supplemental Figure 4).

Hes1 is among the earliest genes upregulated by ectopic activated-Notch1 expression in the developing mouse collecting ducts,[23] and increased Hes1 staining is observed in PCs of SPAK kinase–deficient adult mouse kidneys.[39] Inactivation of *Hes1* in adult mouse collecting ducts and nephrons by providing dox to *Pax8->rtTA; TRE->Cre; Hes1f/f* (*Hes1cKO*) mice from 3 to 5 weeks of age resulted in a severe urine concentrating deficit (Figure 3H), an increase in Atp6v1b1-expressing ICs, and a decrease in Aqp2-expressing PCs (Figure 3, A–F, and I). Consistent with the change in cell types, quantitative RT-PCR using RNA extracts from whole kidneys revealed increased mRNA levels of *Foxi1* and *Atp6v1b1*, and decreased levels of *Aqp2* in *Hes1cKO* kidneys by 1 week after dox treatment (Figure 3).

Segment-Specific Intercalated Cell Types Replace the $Aqp2^+$ Cell Types after Notch Signaling Inhibition in Collecting Ducts and Distal Tubules

ICs are more abundant in the adult kidney collecting ducts after genetic inactivation of Notch signaling. We examined if loss of Notch increases a specific type (A, B, or non-A-non-B) of IC. The type A IC, identified by basolateral expression of the chloride bicarbonate exchanger AE1 and apical expression of the H^+-ATPase pump, is the predominant IC type present in the outer and inner medulla, but not cortex of wild-type kidneys (Figure 4, A, D, and G). Interestingly, it is predominantly the type A IC that is increased in the Notch signaling–deficient OMCD and IMCD segments (Figure 4, E, F, H, and I). Both type B and type non-A-non-B ICs do not express AE1, whereas H^+-ATPase pumps are on the basolateral membrane of type B ICs, and in diffuse vesicles in type non-A-non-B ICs. The type B and non-A-non-B ICs are present predominantly in the cortex of wild-type kidneys (Figure 4A) and are present in increased numbers in the cortex of Notch signaling–deficient cortical tubules (Figure 4, B and C). Pendrin, another marker of type B and non-A-non-B ICs, is mainly present in cortical ICs of wild-type kidneys, and increased in cortical cells of Notch signaling–deficient kidneys (Figure 4, J and K). We did not observe pendrin-positive cells in the OMCDs and IMCDs in the Notch signaling–deficient kidneys (data not shown). Consistent with Notch signaling in adult kidneys preventing expansion of intercalated cell types expressing pendrin (type B and type non-A-non-B) and those expressing AE1 (type A), there is an overall increase in the mRNA levels of *Slc4a1* and *Slc26a4* in the *Hes1*cKO kidneys 1 week after initiation of *Hes1* inactivation (Figure 4L). This trend continues for *Slc26a4* in the *Notch1 & 2cKO* kidneys even 5 weeks after initiation of *Notch1* and *Notch2* inactivation (Figure 4L).

Unlike the collecting ducts, the CNT of the distal nephron, which connects each nephron to the branched collecting duct network, consists of ICs intermingled with a CNT cell type that expresses both Aqp2 and calbindin-D28k (Calb1).[39] Considering that the CNT, along with the rest of the nephron, originate from a lineage distinct from the collecting ducts,[40,41] we examined whether maintenance of $Calb1^+$; $Aqp2^+$ cells in the CNT is also dependent on Notch signaling. Interestingly, the number of $Aqp2^+$ and $Calb1^+$ CNT cells and the number of $Aqp2^-$ and $Calb1^+$ DCT2 cells were decreased in the Notch signaling–deficient kidneys along with an increase in $Atp6v1b1^+$ ICs in these segments (Figure 5D). In wild-type CNTs, each IC is surrounded by $Aqp2^+$ and $Calb1^+$ cells (arrowheads, Figure 5A) whereas in Notch signaling–deficient CNTs, there are many regions containing two or more ICs next to each other (asterisks in Figure 5, B and C) and a reduction in number of $Aqp2^+$ and $Calb1^+$ cells from approximately 65% in wild-type kidneys to about 30% in Notch signaling–deficient kidneys (Figure 5D). The $Aqp2^-$ and $Calb1^+$ DCT2 cells normally comprise 75% of the DCT2 segment, but are reduced to 40%–50% in the Notch signaling–deficient DCT2 segments (Figure 5D). These observations reveal the requirement for *Notch1, Notch2*, and *Hes1* in the maintenance of $Aqp2^+$ and $Calb1^+$, as well as $Aqp2^-$ and $Calb1^+$ epithelial cell types in the distal tubule segments of adult nephrons.

Fate Tracing of Mature PCs in the Inner Stripe of the Outer Medulla Reveals Conversion to Intercalated Cells after Inactivation of *Hes1* and, to Lesser Extent, Lithium Treatment

Loss of Notch signaling in adult kidneys results in increased ICs at the expense of PCs. Although there are several possibilities for increased ICs, one intriguing hypothesis is that PCs convert to ICs. The $Elf5^+$ PC lineage-tracing tool previously described was used to test for direct conversion between cell types.[23] In this system, Elf5 drives rtTA and GFP expression (*Elf5->rtTA;*

Tet-O-Cre; Rosa$^{+/tdtomato}$), and Cre expression in the presence of dox recombines Lox-P sites flanking a transcriptional stop placed upstream of tdtomato coding region at the Rosa locus (Rosa$^{+/tdtomato}$). We have previously observed that mice with *Tet-O-Cre;Rosa*$^{+/tdtomato}$ have a subset of renal interstitial cells labeled with tdtomato independently of inheriting the Elf5-> rtTA transgene. Importantly, only the PCs in the tubular epithelial structures of *Elf5->rtTA;Tet-O-Cre; Rosa*$^{+/tdtomato}$ mice are labeled in a dox-dependent manner, and dox administration does not label renal epithelial cells in *Tet-O-Cre; Rosa*$^{+/tdtomato}$ mice.[23] The Elf5^{+} PCs were labeled with tdtomato in adult mouse kidney collecting ducts by administering dox from 3 to 5 weeks of age (Figure 6A), along with or without inactivation of *Hes1* in *Elf5*-expressing cells, and the fate of tdtomato-labeled PCs was determined at 6 weeks of age. The pattern of tdtomato-labeled collecting duct cells was similar to the expression pattern of *Elf5* in adult kidneys,[23] with the highest labeling in papillary regions, moderate labeling in medullary regions, and minimal labeling in the cortex. When kidneys were stained for either PC marker Aqp4 (Figure 6, B and C) or IC markers c-Kit[22] or Atp6v1b1 (Figure 6, D–G), most (approximately 97%) tdtomato^{+} OMCD cells were Aqp4^{+} (arrowheads in Figure 6B) and almost none (<0.2%) were Atp6v1b1^{+} or c-Kit^{+} (arrowheads in Figure 6, D and F) in wild-type mice 3–5 weeks after initiation of PC labeling. In contrast, a significant number of tdtomato^{+} duct cells begin expressing IC markers 3 weeks after initiation of *Hes1* inactivation in *Elf5*-expressing cells (arrows in Figure 6, E and G), with an average of approximately 40% of tdtomato^{+} OMCD cells expressing IC markers (Figure 6J). An average of 29% of tdtomato^{+} OMCD cells expressing c-Kit still have Aqp4 lingering in the basolateral membranes in Hes1 mutant kidneys (Supplemental Figure 5), whereas 0% of the tdtomato^{+} OMCD cells express both c-Kit and Aqp4 in wild-type kidneys (n=4 control, n=3 Hes1 mutants, at least 100 cells analyzed per mouse). To determine whether the tdtomato^{+} ICs in the *Elf5->rtTA;Tet-O-Cre; Rosa*$^{+/tdtomato}$; *Hes1*$^{f/f}$ mice arise from cells that undergo DNA synthesis and proliferation, we provided BrdU in the drinking water from time of dox treatment to tissue harvest (Figure 6A). Whereas intestinal epithelial cells had BrdU labeling (Supplemental Figure 5A), none of the c-Kit^{+}, Aqp4^{+}, or tdtomato^{+} collecting duct cells in the *Elf5->rtTA;Tet-O-Cre; Rosa*$^{+/tdtomato}$;*Hes1*$^{f/f}$ mice were BrdU-labeled (Supplemental Figure 5). The absence of BrdU labeling within the collecting duct cells implies that they have not undergone DNA synthesis since the initiation of *Hes1* inactivation.

Considering that lithium treatment has been associated with remodeling of the adult collecting ducts and that it is hypothesized that lithium-induced NDI involves PC-to-IC conversion, we used *Elf5->rtTA;Tet-O-Cre; Rosa*$^{+/tdtomato}$ mice to trace the fate of Elf5^{+} OMCD PCs after 2 weeks of lithium treatment (Figure 6A'). Lithium treatment caused a marked drop in urine concentrating capacity and increased number of tdtomato-labeled Atp6v1b1^{+} ICs compared with nonlithium-treated mouse kidneys (data not shown). Two weeks of lithium on average triggers 6% of the tdtomato-labeled PCs in the OMCD to begin expressing IC-specific markers (Figure 6I), which is an increase in PC-to-IC conversion, but is not of statistically significant difference when compared with <0.2% in nonlithium-treated wild-type mice (Figure 6J).

The PC-to-IC Conversion Triggered by Notch Signaling Inactivation in the Adult Kidneys Involves Intermediary Cell States and Upregulation of Foxi1

We next provided BrdU in the drinking water during 2 weeks of dox treatment to 3-week-old *Pax8->rtTA;TRE->Cre;Hes1f/f* mice to determine if cell type conversion required proliferation. Two weeks after initiation of *Hes1* inactivation, the OMCD composition changes from 77% PCs and 23% ICs to 49% PCs, 41% ICs, and 6% PCs and ICs (Figure 7, A–C). Interestingly, although there is almost no incorporation of BrdU in control littermate OMCD cells (average of 0.085%; Figure 7A), 13.8% of OMCD cells are BrdU-labeled with *Hes1* inactivation, of which 10.5% are Aqp4^{+}, 2.3% are c-Kit^{+}, 0.4% are Aqp4^{+} and c-Kit^{+}, and 0.7% are Aqp4^{-} and c-Kit^{-} (Figure 7, B and C). About 95% of the c-Kit^{+} OMCD cells are not BrdU-labeled during 2 weeks after initiation of *Hes1* inactivation, as evidenced by rows of ICs expressing c-Kit that are not BrdU-labeled (Figure 7B). Hence, direct conversion of PC to IC occurs without requiring DNA synthesis. In an attempt to capture the direct conversion, we stained for Aqp4 and Foxi1 using 100-μm-thick kidney sections from *Hes1cKO* mice 1 week after initiation of Hes1 inactivation and from control littermates. Maximum intensity projections (Figure 7, D and E) and 3D reconstructions (Figure 7, F and G, Supplemental Movies 1 and 2) from Z-stack confocal images revealed OMCD cells in the *Hes1cKO* and not in wild-type controls that express both Foxi1 in the nucleus and Aqp4 on the basolateral membrane (asterisks in Figure 7, D–G). Quantification of each cell type per tubule length revealed a significant average increase in intermediate cells (Foxi1^{+} and Aqp4^{+}) along with a significant average reduction of Aqp4^{+} PCs in *Hes1cKO* compared with wild-type mice (Figure 7H).

DISCUSSION

Previous studies have identified a role for Notch signaling in PC fate selection in the developing kidney collecting ducts (Figure 8A).[18,20,23] We have identified a requirement for Notch signaling in the maintenance of mature renal tubular epithelial cell identities in segments with intermingled cells types (Figure 8B). The requirement for Notch signaling in the maintenance of intermingled cell type arrangements in kidney collecting ducts, DCT2 and CNT segments is similar to its requirement in the lung for patterning and maintenance of intermingled club and multiciliated cell types.[42,43] Because *Hes1* inactivation is phenotypically similar to inactivation of *Notch1* and *Notch2* in the adult DCT2, CNTs, and collecting duct

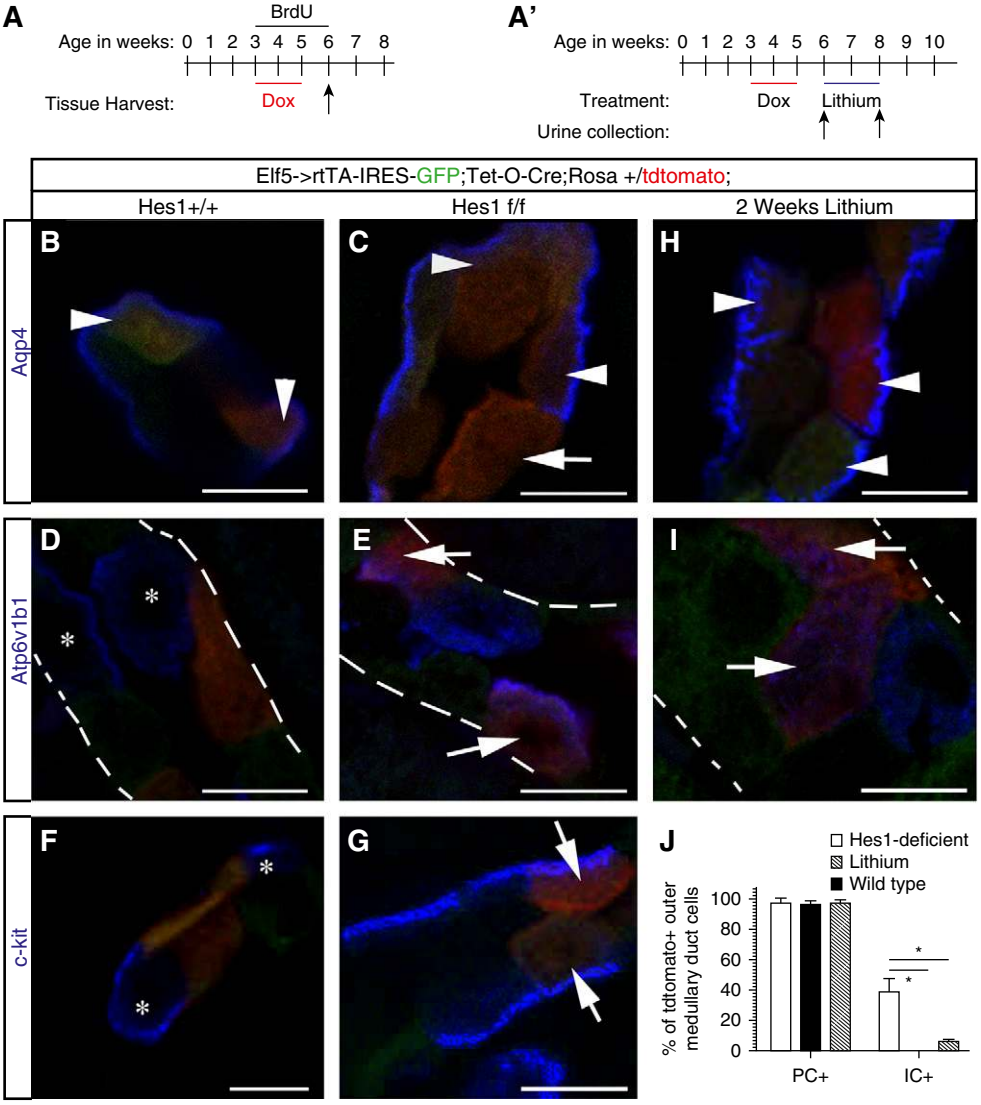

Figure 6. Inhibition of Notch signaling in Elf5^{+} mature PCs triggers a significant increase in principal-to-intercalated cell conversion in the inner stripes of the OMCDs. (A) Dox treatment from 3 to 5 weeks of age pulse-labels a subset of PCs in Elf5->rtTA; Tet-O-Cre; Rosa$^{+/tdtomato}$ mouse kidneys by turning on expression of tdtomato. (B, D, and F) In wild-type OMCD, tdtomato labeling occurs predominantly in cells expressing Aqp4 (arrowheads in B) and tdtomato labeling almost never occurs in intercalated cells expressing Atp6v1b1 (asterisks in D) or c-Kit (asterisks in F). (C, E, and G) Notch signaling inhibition by inducible inactivation of *Hes1* in *Elf5*-expressing PCs shows that some tdtomato-labeled OMCD cells do not express Aqp4 (arrow in C), whereas many other tdtomato-labeled cells still express Aqp4 (arrowheads in C). In the absence of Notch signaling, many of the tdtomato-labeled OMCD cells express intercalated markers Atp6v1b1 (arrows in E) or c-Kit (arrows in G). (A') Schematic of lithium treatment. Dox was administered from 3 to 5 weeks of age to label PCs with tdtomato. Lithium was provided in diet from 6 to 8 weeks of age. Urine was collected before and after lithium treatment. (H and I) Fate tracing of PCs in three *Elf5->rtTA;TRE->Cre; Rosa*$^{+/tdtomato}$ mice treated with lithium for 2 weeks revealed that the labeled cells still mostly remain principal and express Aqp4 (arrowheads in H). However, about 6% of the labeled cells begin expressing intercalated markers, such as Atp6v1b1 (arrows in I). The white dashes in (D, E, and I) outline the borders of OMCDs. (J) Graph showing that about 40% of tdtomato labeled cells in Hes1-deficient inner stripes of the OMCDs begin expressing intercalated cell markers, whereas 6% do so after 2 weeks of lithium treatment and <0.2% do so in wild-type kidneys. *Statistically significant difference between groups as determined by one-way ANOVA (F=25.16; $P<4\times10^{-4}$), and comparing three groups consisting of four wild-type, three Hes1-deficient mice, and three lithium-treated mice. *Post hoc* analysis pairwise comparison using the Tukey method revealed significant differences between wild-type and Hes-1-deficient groups (adjusted $P<2\times10^{-2}$), as well as between lithium-treated and Hes1-deficient groups (adjusted $P<4\times10^{-4}$). Scale bars, 10 μm in (B–I).

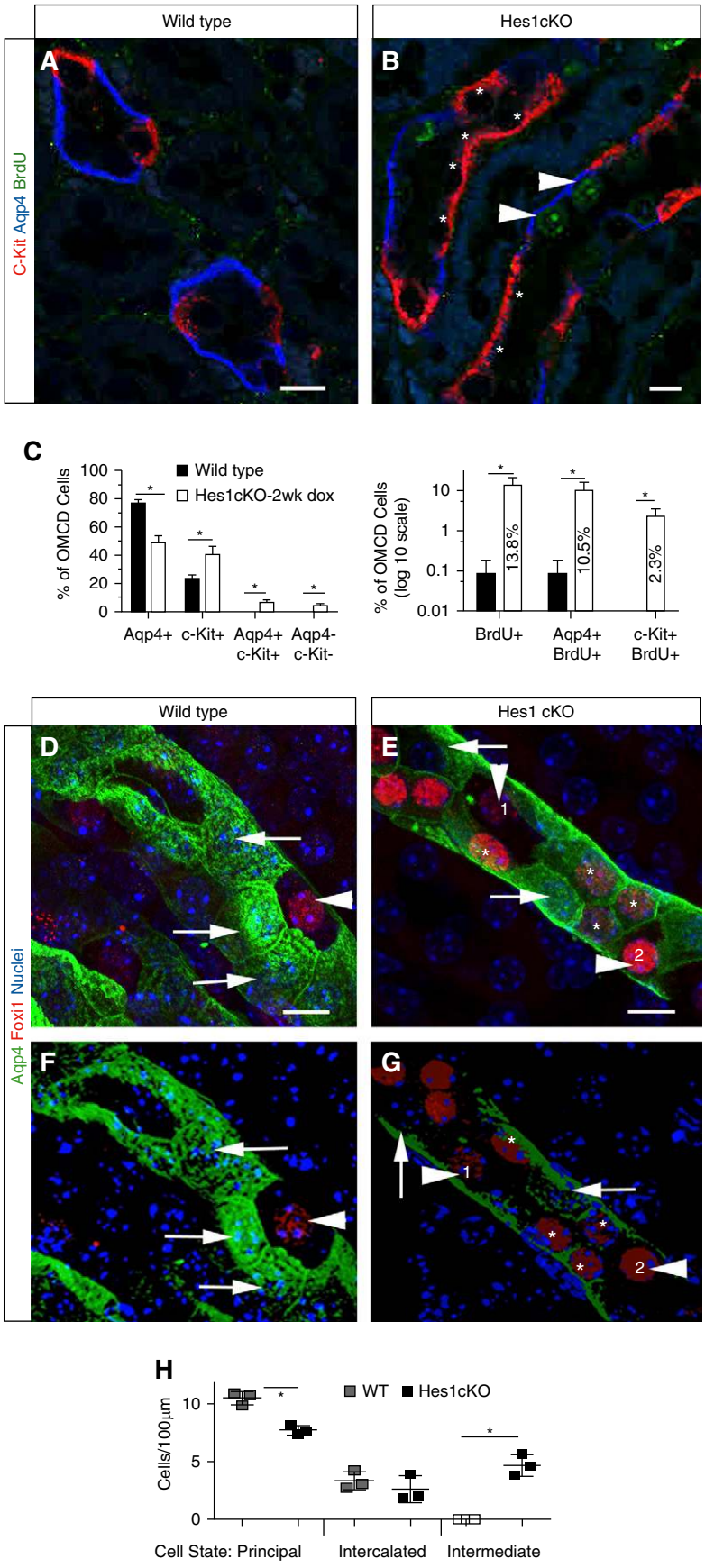

segments, and *Hes1* is a known direct target of Notch signaling, we suggest that Hes1 mediates Notch signaling in Aqp2$^+$ cells to prevent conversion to ICs (Figure 8C). Fate tracing of Elf5$^+$ PCs with inactivation of *Hes1* in the adult inner stripe of the OMCDs revealed that PCs convert to ICs

Figure 7. Principal-to-intercalated cell conversion triggered by inactivation of *Hes1* involves intermediary cell states and upregulation of Foxi1. (A–C) Kidneys from Hes1cKO mice given BrdU in the drinking water during 2 weeks of dox-mediated inactivation of *Hes1* show an increase in the number of BrdU-labeled PCs from 0.1% to about 10% and BrdU-labeled intercalated cells from 0% to 2% (A–C). A majority of the increase in intercalated cells in the inner stripe of the OMCDs from 20% in wild-type to 40% in *Hes1cKO* mice (n=4 per genotype) does not involve BrdU-labeled cells (asterisks in B). In (C), * indicates significant differences by two-tailed unpaired t test when comparing percentages of Aqp4$^+$ (P=6.5×10^{-5}), cKit$^+$ (P=0.001753), Aqp4$^+$ and cKit$^+$ (P=0.007), Aqp4$^-$ and cKit$^-$ (P=0.009), BrdU$^+$ (P=0.04), Aqp4$^+$ and BrdU$^+$ (P=0.04), or cKit$^+$ and BrdU$^+$ (P=0.03) OMCD cells between wild-type and *Hes1cKO* mouse kidneys after 2 weeks of dox treatment (n=4 mice per genotype with at least 1400 OMCD cells analyzed per mouse). (D and E) Maximum intensity projections of confocal Z-stack images (optical sections) captured every 0.175 μm, using a ×60 objective on a Nikon A1 confocal microscope. (F and G) 3D ISO surface images of inner stripes of the OMCD segments generated from Z-stack images using Arivis Vision 4D. (D–G) Different views of a wild-type OMCD segment (D and F) compared with different views of a Hes1cKO OMCD segment (E and G) reveal Foxi1-expressing intercalated cells (arrowheads), Aqp4-expressing PCs (arrows), and intermediate state cells expressing both Foxi1 and Aqp4 (asterisks). The cell labeled 1 is the same cell in (E and G), and similarly the cell labeled 2 is the same cell in (E and G). (H) In the inner stripe of the OMCDs the average number of PCs per tubule length decreases significantly in *Hes1cKO* kidneys compared with wild-type controls. Intermediate cell types are present at significantly higher numbers in the *Hes1cKO* inner stripe of the OMCDs; *P<0.05, when performing unpaired t tests. A minimum of seven OMCD segments were analyzed per mouse, and three mice per genotypic group were analyzed. Scale bars, 10 μm.

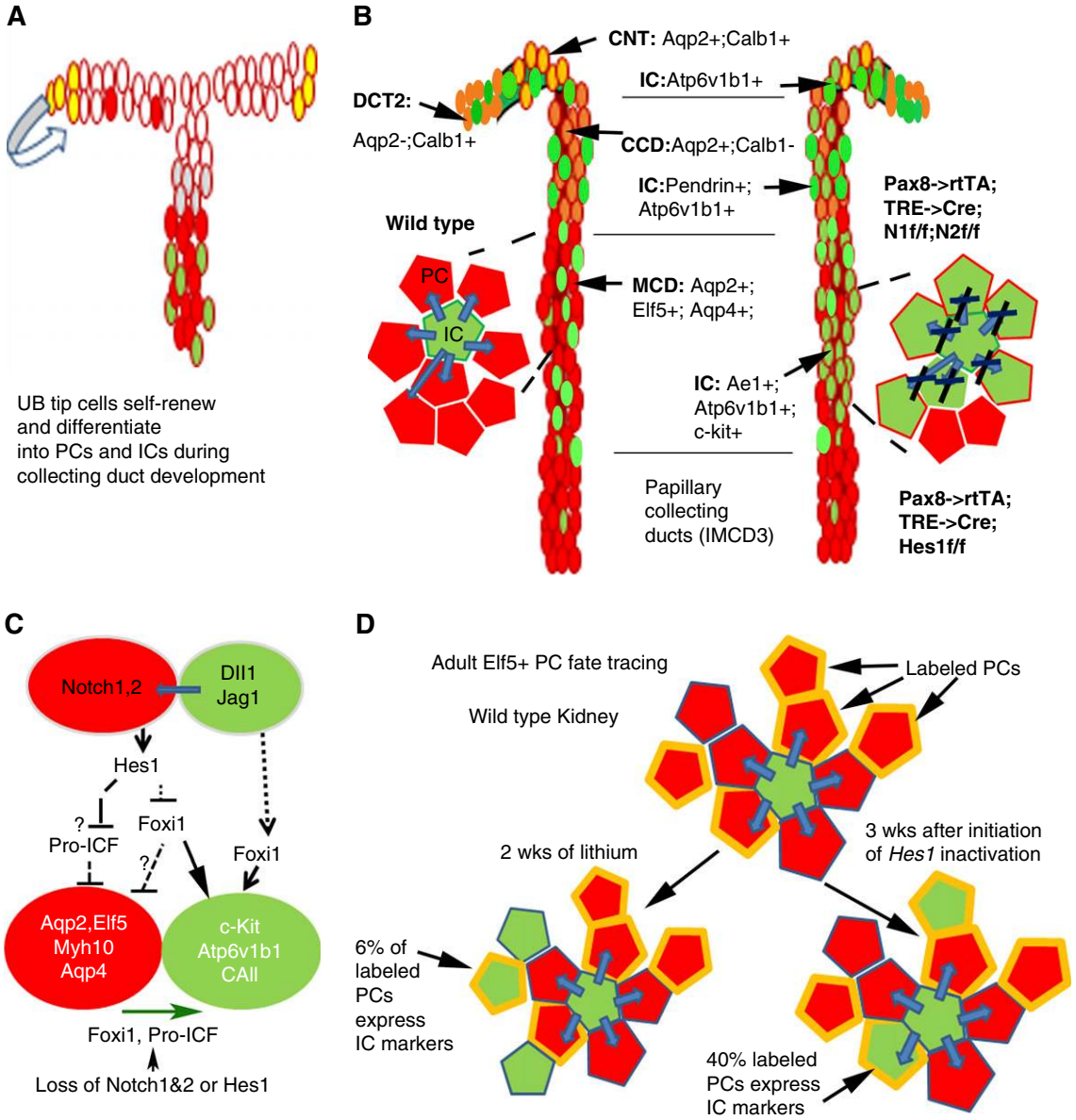

Figure 8. Loss of Notch signaling triggers transdifferentiation of Elf5-expressing epithelial cells and loss of epithelial cell type diversity in the adult kidney CNT and collecting duct segments. (A) Yellow ureteric bud (UB) tip cells self-renew and differentiate into all of the cell types of the collecting ducts. Notch signaling is required for PC fate selection during collecting duct development. (B) Illustration of the cell types found in wild-type versus Notch signaling–deficient adult kidney DCT2, CNT, and collecting duct (CD) segments. Blue arrows indicate the directionality of the Notch signal sending and receiving cells. The segment specific Aqp2-expressing epithelial cells are replaced with segment-specific intercalated cells (ICs) after inactivation of *Notch1* and *Notch2* (N1 and N2) or *Hes1* inactivation in the adult kidney epithelia. (C) Dll1 and Jag1 expressed in ICs activate Notch1 and Notch2 receptor in neighboring cells to maintain the Aqp2-expressing epithelial cell state *via* Hes1 mediated repression of *Foxi1* expression. Inactivation of *Hes1* allows for Foxi1 expression in PCs, and Foxi1 may be sufficient to trigger cell type conversion. Alternatively, Foxi1 may only turn on intercalated cell–specific genes and additional prointercalated cell factors (Pro-ICF), also repressed by Hes1, turn on in the absence of Hes1 to suppress the Aqp2-expressing epithelial cell–specific genes. (D) Fate tracing of genetically labeled adult Elf5-expressing cells (yellow border) indicate that a majority (99.8%) of labeled cells in the inner stripe of the OMCDs express PC markers (red) and do not express IC-markers (green) in adult mice. Two weeks of lithium treatment converts 6% of labeled PCs to ICs, whereas 3 weeks after initiation of *Hes1* inactivation in Elf5-expressing PCs about 40% of labeled PCs express IC markers. MCD, medullary collecting duct cell.

(Figure 8D). This conversion did not require DNA synthesis consistent with a direct conversion of PCs into ICs in absence of Notch signaling. This direct conversion may involve derepression of *Foxi1*, which in turn is capable of activating intercalated cell-specific genes.[44,45] Whether Foxi1 or additional pro-IC factors repressed by Hes1 suppress PC genes

needs to be determined (Figure 8C). The PC-to-IC conversion may involve dot1l, a histone H3-K79-methyltransferase, because inactivation of *dot1l* using *Aqp2-Cre* also increased ICs and decreased PCs.[46] In support of our findings that Notch signaling is required for maintenance of PC state, Park *et al.*[47] report that IC-to-PC transitions occur with ectopic activation of Notch1 and are associated with metabolic acidosis. Additionally, through single-cell RNA-sequencing, they identify individual cells expressing both IC- and PC-specific genes even in normal adult mouse kidneys.[47] Consistent with a low level of constitutive PC-to-IC conversion, we observed $<0.2\%$ of the tdtomato-labeled PCs begin expressing IC markers in wild-type, nonlithium-treated mouse kidneys at 3–5 weeks after initiation of PC labeling.

The question arises as to whether the susceptibility of $Aqp2^+$ cells in the DCT2, CNT of the distal tubules, and the cortical and medullary collecting duct segments to cell type conversion is merely a weakness or if it serves a purpose. On the basis of our observations that short-term lithium triggers a modest $Elf5^+$ PC-to-IC conversion (Figure 8D), and the finding that PC defects occur in the kidneys of patients with bipolar disorder who are prescribed lithium, the plasticity of the PCs appears to be a weakness. However, certain physiologic challenges may require more ICs in the CNT and collecting duct segments, perhaps to maintain pH and electrolyte balance. Along these lines, a low potassium diet is known to trigger an increase in IC-to-PC ratio in the medullary duct.[48,49] Additionally, Notch signaling activation in the distal nephron of SPAK-null mice is associated with cell type remodeling, in which PC numbers increase in the CNT at the expense of type A ICs.[39] This distal nephron remodeling is possibly part of compensatory mechanisms that occur in response to defective NaCl reabsorption in the distal nephron. These observations collectively support the idea that plasticity of the cell types in the CNT and collecting duct segments may allow for physiologic adaptation to electrolyte imbalances.

ACKNOWLEDGMENTS

We thank Ryan Hart for technical assistance and the Molecular Pathology Core, Molecular Biology Core, Imaging Core and COMMAND core for assistance (supported by National Institutes of Health grants P20GM10358, P20GM121341, and P20GM103620).

M.M. and J.d. performed most of the experiments, generated most of the results, and assisted with designing experiments and manuscript preparation. K.O. and I.C. performed immunohistochemistry and imaging for experiments involving analysis of the distal nephron segments, in addition to assisting with manuscript preparation. I.R. and P.A. processed kidneys for TEM and carried out protocol to acquire the TEM images. D.K. processed confocal images to generate 3D-reconstructed images. K.S. designed the experiments and prepared the manuscript.

Research reported here was supported by a grant (to KS) from the National Institute of Diabetes and Digestive and Kidney Diseases, National Institutes of Health under award number R01DK106135.

DISCLOSURES

None.

This article contains the following supplemental material online at http://jasn.asnjournals.org/lookup/suppl/doi:10.1681/ASN.2018040440/-/DCSupplemental.

SUPPLEMENTAL MATERIAL

Supplemental Figure 1. Illustration of the different kidney regions and different collecting duct segments counted.

Supplemental Figure 2. Basescope *in situ* to detect Notch2 mRNA reveals effective inactivation of *Notch2* in the *Pax8rtTA;TRE->;Notch1f/f;Notch2f/f* adult mouse kidneys given dox from 3 to 5 weeks of age, and analyzed at 7 weeks of age.

Supplemental Figure 3. Increased number of OMCD cells with abundant mitochondria in Notch signaling–deficient mouse collecting ducts.

Supplemental Figure 4. Ultrastructure of OMCD cell types.

Supplemental Figure 5. BrdU-labeled intestinal epithelial cells (A), but not the collecting duct epithelia (B and C) during 2 weeks of dox treatment in *Elf5->rtTA;Tet-O-Cre;Hes1f/f;Rosa$^+$/Tdtomato* mice.

Supplemental Table 1. List of transgenic mice.

Supplemental Table 2. List of antibodies.

References for mouse lines and antibodies.

Supplemental Movie 1. 3D reconstruction of wild-type OMCD.

Supplemental Movie 2. 3D reconstruction of Hes1cKO OMCD.

REFERENCES

1. Takahashi K, Yamanaka S: Induced pluripotent stem cells in medicine and biology. *Development* 140: 2457–2461, 2013
2. Alsady M, Baumgarten R, Deen PM, de Groot T: Lithium in the kidney: Friend and foe? *J Am Soc Nephrol* 27: 1587–1595, 2016
3. Trepiccione F, Capasso G, Nielsen S, Christensen BM: Evaluation of cellular plasticity in the collecting duct during recovery from lithium-induced nephrogenic diabetes insipidus. *Am J Physiol Renal Physiol* 305: F919–F929, 2013
4. Little MH, McMahon AP: Mammalian kidney development: Principles, progress, and projections. *Cold Spring Harb Perspect Biol* 4, 2012
5. Brown D, Weyer P, Orci L: Vasopressin stimulates endocytosis in kidney collecting duct principal cells. *Eur J Cell Biol* 46: 336–341, 1988
6. Paragas N, Kulkarni R, Werth M, Schmidt-Ott KM, Forster C, Deng R, et al.: α-Intercalated cells defend the urinary system from bacterial infection. *J Clin Invest* 124: 2963–2976, 2014
7. Brown D, Kumpulainen T: Immunocytochemical localization of carbonic anhydrase on ultrathin frozen sections with protein A-gold. *Histochemistry* 83: 153–158, 1985
8. Bastani B: Immunocytochemical localization of the vacuolar H(+)-ATPase pump in the kidney. *Histol Histopathol* 12: 769–779, 1997
9. Kim J, Tisher CC, Madsen KM: Differentiation of intercalated cells in developing rat kidney: An immunohistochemical study. *Am J Physiol* 266: F977–F990, 1994
10. Emmons C, Kurtz I: Functional characterization of three intercalated cell subtypes in the rabbit outer cortical collecting duct. *J Clin Invest* 93: 417–423, 1994
11. Fejes-Tóth G, Chen WR, Rusvai E, Moser T, Náray-Fejes-Tóth A: Differential expression of AE1 in renal HCO3-secreting and -reabsorbing intercalated cells. *J Biol Chem* 269: 26717–26721, 1994

12. Kim YH, Kwon TH, Frische S, Kim J, Tisher CC, Madsen KM, et al.: Immunocytochemical localization of pendrin in intercalated cell subtypes in rat and mouse kidney. *Am J Physiol Renal Physiol* 283: F744–F754, 2002
13. Teng-umnuay P, Verlander JW, Yuan W, Tisher CC, Madsen KM: Identification of distinct subpopulations of intercalated cells in the mouse collecting duct. *J Am Soc Nephrol* 7: 260–274, 1996
14. Wall SM: Renal intercalated cells and blood pressure regulation. *Kidney Res Clin Pract* 36: 305–317, 2017
15. Brown D, Breton S: Mitochondria-rich, proton-secreting epithelial cells. *J Exp Biol* 199: 2345–2358, 1996
16. Quigley IK, Stubbs JL, Kintner C: Specification of ion transport cells in the Xenopus larval skin. *Development* 138: 705–714, 2011
17. Jänicke M, Carney TJ, Hammerschmidt M: Foxi3 transcription factors and Notch signaling control the formation of skin ionocytes from epidermal precursors of the zebrafish embryo. *Dev Biol* 307: 258–271, 2007
18. Jeong HW, Jeon US, Koo BK, Kim WY, Im SK, Shin J, et al.: Inactivation of Notch signaling in the renal collecting duct causes nephrogenic diabetes insipidus in mice. *J Clin Invest* 119: 3290–3300, 2009
19. Blomqvist SR, Vidarsson H, Fitzgerald S, Johansson BR, Ollerstam A, Brown R, et al.: Distal renal tubular acidosis in mice that lack the forkhead transcription factor Foxi1. *J Clin Invest* 113: 1560–1570, 2004
20. Guo Q, Wang Y, Tripathi P, Manda KR, Mukherjee M, Chaklader M, et al.: Adam10 mediates the choice between principal cells and intercalated cells in the kidney. *J Am Soc Nephrol* 26: 149–159, 2015
21. Werth M, Schmidt-Ott KM, Leete T, Qiu A, Hinze C, Viltard M, et al.: Transcription factor *TFCP2L1* patterns cells in the mouse kidney collecting ducts. *eLife* 6, 2017
22. Chen L, Lee JW, Chou CL, Nair AV, Battistone MA, Păunescu TG, et al.: Transcriptomes of major renal collecting duct cell types in mouse identified by single-cell RNA-seq. *Proc Natl Acad Sci U S A* 114: E9989–E9998, 2017
23. Grassmeyer J, Mukherjee M, deRiso J, Hettinger C, Bailey M, Sinha S, et al.: Elf5 is a principal cell lineage specific transcription factor in the kidney that contributes to Aqp2 and Avpr2 gene expression. *Dev Biol* 424: 77–89, 2017
24. Christensen BM, Marples D, Kim YH, Wang W, Frøkiaer J, Nielsen S: Changes in cellular composition of kidney collecting duct cells in rats with lithium-induced NDI. *Am J Physiol Cell Physiol* 286: C952–C964, 2004
25. Grünfeld JP, Rossier BC: Lithium nephrotoxicity revisited. *Nat Rev Nephrol* 5: 270–276, 2009
26. Wu H, Chen L, Zhou Q, Zhang X, Berger S, Bi J, et al.: Aqp2-expressing cells give rise to renal intercalated cells. *J Am Soc Nephrol* 24: 243–252, 2013
27. Rej S, Pira S, Marshe V, Do A, Elie D, Looper KJ, et al.: Molecular mechanisms in lithium-associated renal disease: A systematic review. *Int Urol Nephrol* 48: 1843–1853, 2016
28. Stratman JL, Barnes WM, Simon TC: Universal PCR genotyping assay that achieves single copy sensitivity with any primer pair. *Transgenic Res* 12: 521–522, 2003
29. Pfaffl MW: A new mathematical model for relative quantification in real-time RT-PCR. *Nucleic Acids Res* 29: e45, 2001
30. Nowotschin S, Xenopoulos P, Schrode N, Hadjantonakis AK: A bright single-cell resolution live imaging reporter of Notch signaling in the mouse. *BMC Dev Biol* 13: 15, 2013
31. Maillard I, Weng AP, Carpenter AC, Rodriguez CG, Sai H, Xu L, et al.: Mastermind critically regulates Notch-mediated lymphoid cell fate decisions. *Blood* 104: 1696–1702, 2004
32. Chang AC, Fu Y, Garside VC, Niessen K, Chang L, Fuller M, et al.: Notch initiates the endothelial-to-mesenchymal transition in the atrioventricular canal through autocrine activation of soluble guanylyl cyclase. *Dev Cell* 21: 288–300, 2011
33. Fu Y, Chang A, Chang L, Niessen K, Eapen S, Setiadi A, et al.: Differential regulation of transforming growth factor beta signaling pathways by Notch in human endothelial cells. *J Biol Chem* 284: 19452–19462, 2009
34. Traykova-Brauch M, Schönig K, Greiner O, Miloud T, Jauch A, Bode M, et al.: An efficient and versatile system for acute and chronic modulation of renal tubular function in transgenic mice. *Nat Med* 14: 979–984, 2008
35. Krebs LT, Deftos ML, Bevan MJ, Gridley T: The Nrarp gene encodes an ankyrin-repeat protein that is transcriptionally regulated by the notch signaling pathway. *Dev Biol* 238: 110–119, 2001
36. Lamar E, Deblandre G, Wettstein D, Gawantka V, Pollet N, Niehrs C, et al.: Nrarp is a novel intracellular component of the Notch signaling pathway. *Genes Dev* 15: 1885–1899, 2001
37. Cheng HT, Kim M, Valerius MT, Surendran K, Schuster-Gossler K, Gossler A, et al.: Notch2, but not Notch1, is required for proximal fate acquisition in the mammalian nephron. *Development* 134: 801–811, 2007
38. Chung E, Deacon P, Marable S, Shin J, Park JS: Notch signaling promotes nephrogenesis by downregulating Six2. *Development* 143: 3907–3913, 2016
39. Grimm PR, Lazo-Fernandez Y, Delpire E, Wall SM, Dorsey SG, Weinman EJ, et al.: Integrated compensatory network is activated in the absence of NCC phosphorylation. *J Clin Invest* 125: 2136–2150, 2015
40. Oxburgh L, Chu GC, Michael SK, Robertson EJ: TGFbeta superfamily signals are required for morphogenesis of the kidney mesenchyme progenitor population. *Development* 131: 4593–4605, 2004
41. Georgas K, Rumballe B, Valerius MT, Chiu HS, Thiagarajan RD, Lesieur E, et al.: Analysis of early nephron patterning reveals a role for distal RV proliferation in fusion to the ureteric tip via a cap mesenchyme-derived connecting segment. *Dev Biol* 332: 273–286, 2009
42. Lafkas D, Shelton A, Chiu C, de Leon Boenig G, Chen Y, Stawicki SS, et al.: Therapeutic antibodies reveal Notch control of transdifferentiation in the adult lung. *Nature* 528: 127–131, 2015
43. Morimoto M, Liu Z, Cheng HT, Winters N, Bader D, Kopan R: Canonical Notch signaling in the developing lung is required for determination of arterial smooth muscle cells and selection of Clara versus ciliated cell fate. *J Cell Sci* 123: 213–224, 2010
44. Kurth I, Hentschke M, Hentschke S, Borgmeyer U, Gal A, Hübner CA: The forkhead transcription factor Foxi1 directly activates the AE4 promoter. *Biochem J* 393: 277–283, 2006
45. Vidarsson H, Westergren R, Heglind M, Blomqvist SR, Breton S, Enerbäck S: The forkhead transcription factor Foxi1 is a master regulator of vacuolar H-ATPase proton pump subunits in the inner ear, kidney and epididymis. *PLoS One* 4: e4471, 2009
46. Xiao Z, Chen L, Zhou Q, Zhang W: Dot1l deficiency leads to increased intercalated cells and upregulation of V-ATPase B1 in mice. *Exp Cell Res* 344: 167–175, 2016
47. Park J, Shrestha R, Qiu C, Kondo A, Huang S, Werth M, et al.: Single-cell transcriptomics of the mouse kidney reveals potential cellular targets of kidney disease. *Science* 360: 758–763, 2018
48. Park EY, Kim WY, Kim YM, Lee JH, Han KH, Weiner ID, et al.: Proposed mechanism in the change of cellular composition in the outer medullary collecting duct during potassium homeostasis. *Histol Histopathol* 27: 1559–1577, 2012
49. Kim WY, Nam SA, Choi A, Kim YM, Park SH, Kim YK, et al.: Aquaporin 2-labeled cells differentiate to intercalated cells in response to potassium depletion. *Histochem Cell Biol* 145: 17–24, 2016

AFFILIATIONS

[1]Pediatrics and Rare Diseases Group and [2]Enabling Technologies Group, Sanford Research, Sioux Falls, South Dakota; [3]Department of Nanoscience and Nanoengineering, South Dakota School of Mines and Technology, Rapid City, South Dakota; and [4]Department of Pediatrics, Sanford School of Medicine, University of South Dakota, Sioux Falls, South Dakota